Toward Predictive Modeling of Full-Size Packages with Layered-Medium Integral-Equation Methods

C. Liu[1], A. Menshov[1], V. Subramanian[1], K. Aygün[2], H. Braunisch[2], V. I. Okhmatovski[3], and A. E. Yılmaz[1]
[1]Department of Electrical and Computer Engineering, The University of Texas at Austin, Austin, Texas, USA
[2]Intel Corporation, Chandler, Arizona, USA
[3]Department of Electrical and Computer Engineering, University of Manitoba, Winnipeg, Manitoba, Canada

***Abstract*—Layered-medium integral-equation (LMIE) methods that can confront the multiscale problems encountered in electromagnetic modeling of electronic packages are presented. The methods include (i) an impedance-boundary condition (IBC) formulation for modeling conductor thickness, roughness, and finite conductivity, (ii) non-radiating lumped-port models for extracting network parameters, and (iii) FFT based iterative and hierarchical-matrix ($\mathcal{H}$ -matrix) based direct algorithms for efficiently solving the resulting systems of equations. The methods are used to analyze increasingly higher fidelity models of a benchmark packaging interconnect structure; the results are validated with measurements; and the tradeoff between increased model fidelity and computational costs are quantified.**

Keywords—integral-equation methods; layered media; multiscale analysis; fast algorithms

I. INTRODUCTION

Predictive electromagnetic modeling of electronic packages for signal integrity, noise mitigation, and power delivery is a challenging multiscale problem [1], where important field variations are observed in the domain of analysis at multiple length scales. Because both the interconnect structures (signal nets, ground/power/dummy metals, vias, etc.) and the background medium they occupy (package build-up layers, solder resist, etc.) consist of significant features at different length scales, electromagnetic modeling of electronic packages can be categorized as a Type 4 (*multiscale-squared*) multiscale problem [2]. As a result of the "tyranny of scales," all computational methods to solve the governing equations quickly run into accuracy, efficiency, and scalability limitations and eventually break down as the size and fidelity of package models increase. LMIE methods offer a promising avenue to reach full-size and high-fidelity simulations of packages because they can (i) address multiscale background features through Green's functions [3]—and avoid solving for complex field distributions in the substrate or in artificial absorbing layers introduced to truncate the model—(ii) approximate field variations inside conductors by resorting to a range of (low-dimensional) surface-based models [4], [5], and (iii) solve the dense, large, often poorly conditioned but non-arbitrary systems of equations resulting from the discretization of LMIEs by using advanced iterative [6]–[8] and direct [9], [10] solvers accelerated by physics-based algorithms.

In this article, the potential of LMIE methods for predictive modeling of packages is demonstrated by (i) computing the *S*-parameters of a benchmark packaging interconnect structure using increasingly higher fidelity models, (ii) contrasting the computed results to each other and to measurements, and (iii) quantifying the corresponding computational costs. The results show that the parameters found using higher-fidelity models agree more closely with the measured ones and that an IBC, non-radiating lumped port models, and preconditioned fast iterative or fast direct algorithms are necessary ingredients for predictive modeling of full-size packages.

II. LMIE METHODS

Consider extraction of network parameters for a structure composed of metallic conductors in a planar layered medium terminated at P electrically small ports. At each frequency of interest, the port currents are computed in response to P different excitations: For each excitation i, port i is driven by a 1 V time-harmonic voltage source while the other ports are shorted. LMIEs are formulated by enforcing (i) the line integral of the electric field across each port to be 1 V or zero and (ii) an IBC that links fields tangential to conductor surfaces S:

$$\begin{aligned} &\int_{\mathbf{r}=\mathbf{r}_p^+}^{\mathbf{r}=\mathbf{r}_p^+ + h_p\hat{h}_p} \mathcal{L}(\mathbf{J},\mathbf{r})\cdot\hat{h}_p dh = \delta_{pi} \qquad \forall \mathbf{r}_p^+ \in L_p^+ \\ &\hat{n}\times\hat{n}\times\mathcal{L}(\mathbf{J},\mathbf{r}) - Z_s\mathbf{J}(\mathbf{r}) = 0 \qquad \forall \mathbf{r}\in S \end{aligned} \tag{1}$$

Here, each port $p\in\{1,\ldots,P\}$ is modeled as a rectangular surface, $\hat{h}_p$ is the unit vector that points from the port's higher-potential edge L_p^+ to its lower-potential edge h_p away [11], $\mathbf{r}_p^+$ is a point on L_p^+, and δ is the Kronecker delta. In (1), Z_s is a surface impedance term, $\hat{n}$ is the outward-pointing unit normal on S, and the operator $\mathcal{L}$ in mixed-potential form is

$$\mathcal{L}(\mathbf{J},\mathbf{r}) = -j\omega\iint_S \underline{\underline{\mathbf{K}}}(\mathbf{r},\mathbf{r}')\mu_0\mathbf{J}(\mathbf{r}')ds' + \nabla\iint_S g^{\phi}(\mathbf{r},\mathbf{r}')\frac{\nabla'\cdot\mathbf{J}(\mathbf{r}')}{j\omega\varepsilon_0}ds' \tag{2}$$

Here, g^{ϕ} and $\underline{\underline{\mathbf{K}}} = \hat{x}\hat{x}K^{xx} + \hat{x}\hat{z}K^{xz} + \hat{y}\hat{y}K^{yy} + \hat{y}\hat{z}K^{yz} + \hat{z}\hat{x}K^{zx} + \hat{z}\hat{y}K^{zy} + \hat{z}\hat{z}K^{zz}$ are corrected scalar and dyadic Green functions (formulation C in [3]). In general, the Green functions must be calculated using Sommerfeld integrals and transmission-line theory [3]; here, these integrals are accelerated by spectral asymptotic term extraction and are interpolated spatially [7].

The LMIEs in (1) are discretized via the method of moments (MoM): (i) S is meshed into triangular patches with N_S internal edges, (ii) $2N_{\text{port}}$ triangle edges at the P ports are labeled as port edges, (iii) the unknown surface current density $\mathbf{J}$ is expanded using N_S RWG [12] and N_{port} port basis functions, each of which consist of two *disconnected* half RWG functions (the current across the port surface does not radiate); and (iv) (1) is Petrov-Galerkin tested with N_S RWG and N_{port} port testing functions, which enforces the average line integral of the electric field across each port to be equal to 1 V or zero [11]. This yields the system of equations $\mathbf{ZI} = \mathbf{V}$, where

$$\mathbf{Z}_{N\times N} = \begin{bmatrix} \mathbf{Z}^{\text{port,port}}_{N_{\text{port}}\times N_{\text{port}}} & \mathbf{Z}^{\text{port,S}}_{N_{\text{port}}\times N_S} \\ \mathbf{Z}^{\text{S,port}}_{N_S\times N_{\text{port}}} & \mathbf{Z}^{\text{S,S}}_{N_S\times N_S} \end{bmatrix} \quad \begin{aligned} \mathbf{I}_{N\times P} &= [\,\mathbf{I}_1 \;\; \dots \;\; \mathbf{I}_P\,] \\ \mathbf{V}_{N\times P} &= [\,\mathbf{V}_1 \;\; \dots \;\; \mathbf{V}_P\,] \end{aligned} \tag{3}$$

The interactions among all basis-testing function pairs are in the dense $N\times N$ impedance matrix $\mathbf{Z}$ while the unknown current coefficients and the port voltages for the i^{th} excitation are in the $N\times 1$ column vector $\mathbf{I}_i$ and the first N_{port} rows of $\mathbf{V}_i$.

The computation time and memory requirement of the MoM procedure are reduced by adopting an FFT-based fast iterative solver [6]–[8] combined with the 'element-diagonal pre-conditioner' [13] and an $\mathcal{H}$-matrix based fast direct solver [9], [14]. The fast iterative solver embeds the structure in a regular grid of $N_C = N_{xy}\times N_z$ nodes and approximates the impedance matrix as $\mathbf{Z} \approx \mathbf{Z}^{\text{corr}} + \mathbf{Z}^{\text{FFT}}$, where $\mathbf{Z}^{\text{corr}}$ is a sparse matrix to pre-correct interactions between geometrically close basis-testing function pairs and $\mathbf{Z}^{\text{FFT}}$ is the multiplication of sparse inter-/anter-polation matrices and a set of two-level block-Toeplitz (in x,y directions) grid-to-grid propagation matrices. Using 2-D FFTs and precomputing the FFTs for the propagation matrices, $\mathcal{O}(N_{\text{near}} + N_z^2 N_{xy}\log N_{xy})$ operations are required for the matrix-fill stage and (3) can be solved in $\mathcal{O}(P\bar{N}_{\text{iter}}[N_{\text{near}} + N_z N_{xy}\log N_{xy} + N_z^2 N_{xy}])$ operations, where N_{near} is the number of pre-corrected interactions and $\bar{N}_{\text{iter}}$ is the average number of iterations per excitation. When P or $\bar{N}_{\text{iter}}$ is large, direct solution methods, which require $\mathcal{O}(N\log^2 N)$ operations to fill and factorize the impedance matrix (in a low-rank/ compressed manner) for structures of electrically moderate size, such as electronic packages below 40 GHz, become more attractive. In this article, the factorization is calculated and stored in compressed $\mathcal{H}$-form [9], [14] using $\mathcal{H}$-arithmetic with a singular-value-decomposition tolerance of τ_{SVD} and the solution is obtained for each excitation via $\mathcal{H}$-back substitution.

III. Benchmark Interconnect Problem

To demonstrate the potential of the above LMIE methods for package analysis, a two-port interconnect structure is analyzed. In this structure, the two ends of a package microstrip signal line are coupled to two microprobe launcher structures that connect to the ground plane by cylindrical vias; the *S*-parameters of the interconnect are measured by driving it with ground-signal-ground type microprobes [15]. Five different models of the structure are used to compute the network parameters (Fig. 1).

For the simplest model I, the signal line and the ground plane are modeled as two perfect electrically conducting (PEC) thin sheets and the launchers are simplified as two vertical ports connecting the ends of the signal line to the ground plane. The

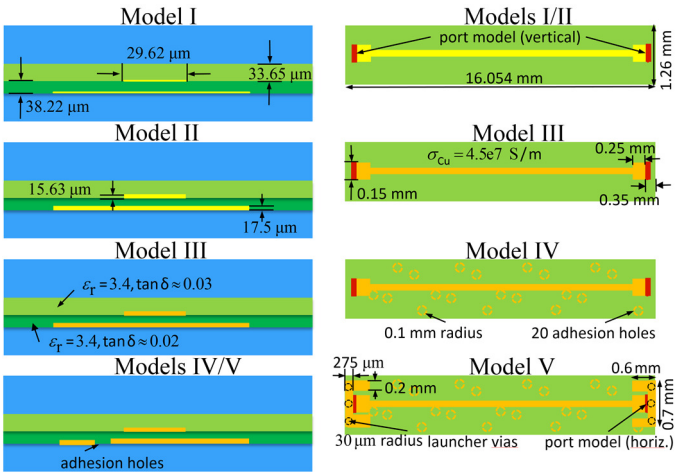

Figure 1. Cross-section (left) and top-down (right) views of the different models for the benchmark problem. (Yellow: PEC; orange: IBC; light green: solder resist; dark green: dielectric substrate; red: port location.)

height and electromagnetic properties of the layers are the same in all models; in particular, both dielectrics are assigned the relative permittivity $\varepsilon_r = 3.4$ and loss tangents that are within $\mp 10\%$ of the values specified in Fig. 1. In model II, conductor thickness is considered by meshing all the surfaces of the signal line and ground plane. The ports now connect the bottom surface of the signal line and the top surface of the ground plane. In model III, the finite conductivity and surface roughness of the conductors are modeled via the IBC. Specifically, $Z_s = (1+j)/\delta_{\text{Cu}}\sigma_{\text{Cu}}$ is used, where δ_{Cu} is the skin depth and σ_{Cu} is the conductivity of copper. To account for the conductor surface roughness, the surface impedance is multiplied with the Groiss correction factor [16] found using an RMS roughness value of $0.3\ \mu\text{m}$; various other surface roughness models could also be used [17], [18]. In model IV, adhesion holes are added to the ground plane. In the most complete model V, launchers including their three grounded vias are added. The port surfaces are now oriented horizontally and are between the bottom of the signal line and the launchers. The triangular mesh for the highest fidelity model is shown in Fig. 2. The models resulted in $N = 7856$ to $N = 14\,973$ unknowns.

The *S*-parameters obtained from the different fidelity models using an iterative MoM solver are compared to those obtained from measurements in Fig. 3. The simulation results are broadly consistent with each other and the measured data; moreover, the *S*-parameters obtained from higher-fidelity models are observed to correlate better with those from measurements. Fig. 3 shows that modeling conductor thickness can be beneficial even for PEC models, especially below 15 GHz for S_{11} and throughout the band for S_{12} (in the sense that peaks and dips correlate better with measurements), but requires significant additional computational resources (model I vs. II results). The figure also shows the necessity of modeling conductor losses, especially for S_{12} results (model I-II vs. III-V results). Results agree poorly below 3 GHz for S_{11} due to measurement limitations as well as the unsuitability of the IBC in (1). Although the *S*-parameters and computational costs for models III-V appear similar when compared to those from model I, model V results agree best with the measurements (except for S_{12} in the 20-25 GHz range) and are the most costly to obtain, e.g., the matrix-solve times are significantly larger due to poorer matrix conditioning.

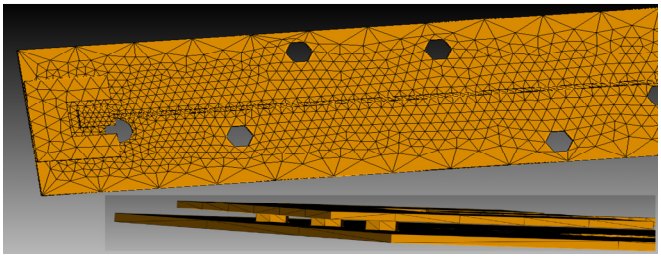

Figure 2. Part of the triangular mesh for model V showing adhesion holes, one of the launchers, conductor side walls, and launcher vias (zoomed view).

Model IV was also simulated using the FFT-based fast iterative solver ($120\times15\times8$ node auxiliary grid, third-order polynomial interpolation, and three-cell pre-correction region) and the $\mathcal{H}$-matrix based direct solver ($\tau_{\text{SVD}} = 10^{-3}$). The resulting S_{11} parameters were within 0.5 dB of the ones in Fig. 3 at all frequencies. At 40 GHz, the fast iterative solver required $\sim 390\,\text{MB}$ of memory, $\sim 10^4\,\text{s}$ for matrix-fill time, and $\sim 150\,\text{s}$ for matrix-solve time; the fast direct solver required $\sim 320\,\text{MB}$ of memory after compression, $\sim 8\times10^4\,\text{s}$ for the matrix-fill time including the time for low-rank approximations, $\sim 14\,\text{s}$ for matrix-factorize time, and $\sim 0.1\,\text{s}$ for matrix-solve time.

IV. Conclusion

The LMIE methods summarized in this article, while necessary ingredients, are not sufficient for full-size package analysis. The results, however, indicate that LMIE methods can be scaled up to combat the multiscale challenges posed by the analysis of full-scale electronic packages; specifically, integration with recently introduced (i) 3D-FFT based algorithms [7], [8] and more advanced pre-conditioners [19] for accelerating the iterative solution, (ii) regular-grid based compression algorithms for accelerating the direct solution [20], and (iii) parallelization of these methods on heterogeneous clusters [21], are expected to be the key remaining ingredients.

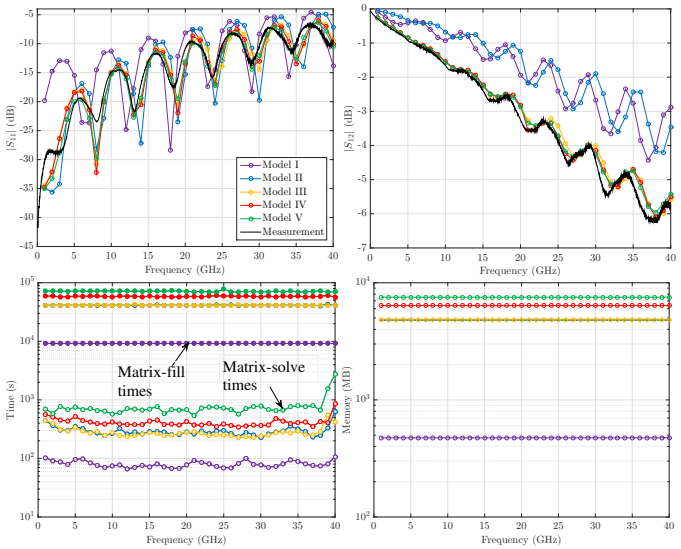

Figure 3. Top: *S*-parameters obtained from the five models vs. measured ones. Bottom: Corresponding time and memory costs using a pre-conditioned [13] but unaccelerated iterative MoM solver.

References

[1] W. C. Chew *et al.*, "Fast and accurate multiscale electromagnetic modeling framework: an overview," in *Proc. 17th IEEE W. Signal Power Int. (SPI)*, May 2013.

[2] Y. Brick, J. W. Massey, K. Yang, and A. E. Yilmaz, "All multiscale problems are hard, some are harder—a nomenclature for classifying multiscale electromagnetic problems," in *Proc. USNC/URSI Rad. Sci. Meet.*, July 2016.

[3] K. A. Michalski and D. Zheng, "Electromagnetic scattering and radiation by surfaces of arbitrary shape in layered media, Part I: theory," *IEEE Trans. Antennas Propag.*, vol. 38, no. 3, pp. 335–344, Mar. 1990.

[4] Z. G. Qian, W. C. Chew, and R. Suaya, "Generalized impedance boundary condition for conductor modeling in surface integral equation," *IEEE Trans. Microw. Theory Techn.*, vol. 55, no. 11, pp. 2354–2364, Nov. 2007.

[5] J. D. Morsey, V. I. Okhmatovski, and A. C. Cangellaris, "Finite-thickness conductor models for full-wave analysis of interconnects with a fast integral equation method," *IEEE Trans. Adv. Packag.*, vol. 27, no. 1, pp. 24–33, Feb. 2004.

[6] V. Okhmatovski, M. Yuan, I. Jeffrey, and R. Phelps, "A three-dimensional precorrected FFT algorithm for fast method of moments solutions of the mixed-potential integral equation in layered media," *IEEE Trans. Microw. Theory Techn.*, vol. 57, no. 12, pp. 3505–3517, Nov. 2009.

[7] K. Yang and A. E. Yılmaz, "A three dimensional adaptive integral method for scattering from structures embedded in layered media," *IEEE Trans. Geosci. Remote Sens.*, vol. 50, no. 4, pp. 1130–1139, Apr. 2012.

[8] K. Yang and A. E. Yılmaz, "FFT-accelerated analysis of scattering from 3D structures residing in multiple layers," in *Proc. Comp. Electromagn. Int. Workshop*, Aug. 2013.

[9] A. Menshov, K. Yang, V. Okhmatovski, and A. Yılmaz, "An $\mathcal{H}$-matrix accelerated direct solver for fast analysis of scattering from structures in layered media," in *Proc. USNC/URSI Rad. Sci. Meet.*, July 2015.

[10] Y. Brick, V. Subramanian, and A. E. Yilmaz, "Rank deficiency of impedance matrix blocks for layered media," in *Proc. USNC/URSI Rad. Sci. Meet.*, July 2015.

[11] J. W. Massey, V. Subramanian, C. Liu, and A. E. Yılmaz, "Analyzing UHF-band antennas near anatomical human models with a fast integral-equation method," in *Proc. Euro. Conf. Ant. Propag. (EuCAP)*, 2016.

[12] S. M. Rao, D. R. Wilton, and A. W. Glisson, "Electromagnetic scattering by surfaces of arbitrary shapes," *IEEE Trans. Antennas Propag.*, vol. 30, no. 3, pp. 409–418, May 1982.

[13] J. Aronsson, M. Shafieipour, and V. Okhmatovski, "Study of pre-conditioners for RWG MoM analysis of large scale scatterers containing junctions with open surfaces and delta-gap voltage sources," in *Proc. Appl. Comp. Electromagn. Symp.*, Apr. 2012.

[14] W. Hackbusch, "A sparse matrix arithmetic based on $\mathcal{H}$-matrices. I. Introduction to $\mathcal{H}$-matrices," *Computing*, vol. 62, pp. 89–108, 1999.

[15] H. Braunisch, X. Gu, A. Camacho-Bragado, and L. Tsang, "Off-chip rough-metal-surface propagation loss modeling and correlation with measurements," in *Proc. ECTC*, pp. 785–791, June 2007.

[16] S. Groiss, I. Bardi, O. Biro, K. Preis, and K. R. Richter, "Parameters of lossy cavity resonators calculated by the finite element method," *IEEE Trans. Magn.*, vol. 32, no. 3, pp. 894-897, May 1996.

[17] B. Curran, I. Ndip, S. Guttowski, and H. Reichl, "A methodoloy for combined modeling of skin, proximity, edge, and surface roughness effects," *IEEE Trans. Microw. Theory Techn.*, vol. 58, no. 9, pp. 2448–2455, Sep. 2010.

[18] G. Gold and K. Helmreich, "A physical model for skin effect in rough surfaces," in *Proc. 42nd EuMC*, pp. 1011–1014, Oct. 2012.

[19] V. Okhmatovski, C. Liu, A. Menshov, and A. E. Yılmaz, "A multiplicative Calderon preconditioner for the impedance boundary condition electric field integral equation," in *Proc. USNC/URSI Rad. Sci. Meet.*, July 2016.

[20] A. Menshov, Y. Brick, and A. E. Yılmaz, "A fast direct integral-equation solver for hydraulic fracture diagnosis," in *Proc. USNC/URSI Rad. Sci. Meet.*, July 2016.

[21] J. W. Massey, A. Menshov, and A. E. Yılmaz, "An empirical methodology for judging the performance of parallel algorithms on heterogeneous clusters," in *Proc. 13th Int. W. Finite Elem. Microw. Eng.*, May 2016.

This work was supported by Intel Corporation.